

Studying the Chiral Magnetic Effect in Pb-Pb and Xe-Xe collisions using the AVFD model

Shi Qiu^{1,2,*}

¹Nikhef

²Utrecht University

Abstract. Quantum Chromodynamics permits the formation of charge conjugation parity violating domains inside the medium produced in heavy-ion collisions, resulting in an imbalanced quark chirality. With the presence of a strong magnetic field (as strong as 10^{15} T) produced by the spectator protons in off-central heavy-ion collisions, this would lead to an electric-charge separation along the direction of the magnetic field, known as the Chiral Magnetic Effect (CME). Experimental searches commonly utilise strategies involving charge-dependent correlators to measure the charge separation. These correlators are, however, dominated by a large background proportional to the elliptic flow v_2 . This article presents a systematic study of the correlators used experimentally to probe the CME by using the Anomalous Viscous Fluid Dynamics (AVFD) model in Pb-Pb and Xe-Xe collisions at $\sqrt{s_{NN}} = 5.02$ TeV and $\sqrt{s_{NN}} = 5.44$ TeV, respectively. The results from AVFD suggest that Xe-Xe collisions are consistent with a background-only scenario and a significant non-zero value of axial current density (imbalanced quark chirality) is required to describe the measurements in Pb-Pb collisions.

1 Introduction

The topologically non-trivial configurations of QCD vacuum can give rise to domains of net chirality [1, 2]. In the presence of chirality imbalance, the chiral magnetic effect (CME) was proposed to occur in non-central heavy-ion collisions with sufficiently large magnetic fields created by the fast, oppositely directed spectator protons [3, 4]. Theoretical calculation suggests that the strength of the magnetic field can be of order of $eB \sim 10^{15}$ T [5–7]. Albeit decaying fast in time, the magnetic field aligns the quarks' spin preferably along the magnetic field direction and the momentum direction of quarks with specific chirality aligns accordingly to their spin orientation. This leads to a global electric charge separation with respect to the reaction plane defined by the impact parameter and the beam axis, with the strength of the charge separation proportional to the amount of chirality imbalance and the strength of the magnetic field. The discovery of the chiral magnetic effect may serve as a sign of the local P (parity) and CP (charge conjugation parity) violation in QCD.

Experimentally, the signature of charge separation can be measured through charge-dependent azimuthal correlations, to be introduced in the next section, relative to the reaction plane [8]. The ALICE collaboration has reported the measurements for Pb–Pb and

*e-mail: s.qiu@nikhef.nl

Xe–Xe collisions at $\sqrt{s_{NN}} = 2.76$ and 5.02 TeV (for Pb ions) [9, 10] and at $\sqrt{s_{NN}} = 5.44$ TeV (for Xe ions) [11, 12], in which the results were aligned with initial expectations for a charge separation with respect to the reaction plane due to the CME. However, the observation of quantitative agreement between the same charge-dependent correlations in the LHC and the RHIC [13, 14], despite of different collision energies and collision systems leading to different multiplicity densities and magnetic fields, hints that these correlations are heavily contaminated by background effects. The sources of contamination were identified to be mainly from local charge conservation coupled to the anisotropic expansion of the system in non-central collisions [15, 16]. Overall, the disentanglement of the CME signal from the background effects has been exceptionally challenging.

In this article we perform a systematic study of the measurements of the correlators used in CME searches reported by the ALICE collaboration for Pb–Pb and Xe–Xe collisions at $\sqrt{s_{NN}} = 5.02$ TeV (for Pb ions) [10] and at $\sqrt{s_{NN}} = 5.44$ TeV (for Xe ions) [11, 12] with the Anomalous-Viscous Fluid Dynamics (AVFD) framework [17–19]. AVFD is a state-of-the-art model which simulates the heavy-ion collisions based on the Glauber initial conditions followed by 2+1 dimensional viscous hydrodynamics (VISH2+1) and a hadron cascade model (UrQMD) with additionally implementing the development of the early stage electromagnetic fields as well as the propagation of anomalous fermion currents in the QGP.

2 Charge-dependent azimuthal correlators

The three-particle charge-dependent azimuthal correlator proposed to be sensitive to charge separation with respect to the reaction plane, known as $\gamma_{1,1}$, is defined as

$$\begin{aligned}\gamma_{1,1} &= \langle \cos(\varphi_\alpha + \varphi_\beta - 2\Psi_{RP}) \rangle = \langle \cos[(\varphi_\alpha - \Psi_{RP}) + (\varphi_\beta - \Psi_{RP})] \rangle \\ &= \langle \cos(\Delta\varphi_\alpha + \Delta\varphi_\beta) \rangle = \langle \cos\Delta\varphi_\alpha \cos\Delta\varphi_\beta \rangle - \langle \sin\Delta\varphi_\alpha \sin\Delta\varphi_\beta \rangle \\ &= \langle v_{1,\alpha}v_{1,\beta} \rangle + B_{in} - \langle a_{1,\alpha}a_{1,\beta} \rangle - B_{out},\end{aligned}\quad (1)$$

where φ represents the azimuthal angle of a track while α and β indicate either same or opposite charges combinations. The decomposed terms $\langle \cos\Delta\varphi_\alpha \cos\Delta\varphi_\beta \rangle$ and $\langle \sin\Delta\varphi_\alpha \sin\Delta\varphi_\beta \rangle$ quantify the correlations with respect to the in- and out-of-plane directions, respectively. The final expression reflects the correlations along the axis in the reaction plane (directed flow, $\langle v_{1,\alpha}v_{1,\beta} \rangle$) and the axis perpendicular to the reaction plane (P-odd terms, $\langle a_{1,\alpha}a_{1,\beta} \rangle$). The parity-conserving correlations projected onto the in- (B_{in}) and out-of-plane (B_{out}) directions significantly cancel out when taking the difference of opposite-sign $\gamma_{1,1}$ (OS) and same-sign pairs $\gamma_{1,1}$ (SS) as our final observable for CME ($\Delta\gamma$).

In addition, a genuine two-particle correlation without dependence on any symmetry plane can be defined as

$$\begin{aligned}\delta_1 &= \langle \cos(\varphi_\alpha - \varphi_\beta) \rangle = \langle \cos[(\varphi_\alpha - \Psi_{RP}) - (\varphi_\beta - \Psi_{RP})] \rangle \\ &= \langle \cos(\Delta\varphi_\alpha - \Delta\varphi_\beta) \rangle = \langle \cos\Delta\varphi_\alpha \cos\Delta\varphi_\beta \rangle + \langle \sin\Delta\varphi_\alpha \sin\Delta\varphi_\beta \rangle \\ &= \langle v_{1,\alpha}v_{1,\beta} \rangle + B_{in} + \langle a_{1,\alpha}a_{1,\beta} \rangle + B_{out},\end{aligned}\quad (2)$$

which is dominated by non-flow effects caused by streams of charged particles flying in the same direction due the physical processes such as resonance decays, jets and transverse momentum conservation. The combination of the δ_1 and $\gamma_{1,1}$ correlators makes it possible to separately quantify the magnitude of correlations in- and out-of-plane.

3 Model parametrisation

In the AVFD model, two key parameters are used to control the CME signal and the background, respectively. The former is governed by the axial charge density, denoted as n_5/s , representing the imbalance between left- and right-handed fermions. The parameter which controls the background is the percentage of local charge conservation (LCC) within an event. This number can be considered as the amount of positive and negative charged partners emitted from the same fluid element at the freeze-out, relative to the total multiplicity of the event. Our goal is to utilise AVFD to parameterise the dependence of $\Delta\delta_1$ and $\Delta\gamma_{1,1}$ at each chosen centrality bin with respect to the axial charge density and the percentage of local charge conservation, respectively. The parametrisation allows us to find the optimum values of n_5/s and LCC to best describe simultaneously the centrality dependence of the charge-dependent correlations, $\Delta\delta$ and $\Delta\gamma$, measured in both Pb-Pb and Xe-Xe collisions.

The calibration of the AVFD model to reproduce the charged particle multiplicity density, charged particle p_T spectra and elliptic flow v_2 of both Pb-Pb and Xe-Xe collisions is summarised in section 3 of [20]. New AVFD samples were produced for centralities ranging from 0 to 70 with 7 equal intervals, for both systems and energies. The baseline sample has n_5/s and LCC both set to zero. Then, the amount of CME induced signal was incremented i.e., using $n_5/s = 0.05, 0.07$ and 0.1 , while the percentage of LCC was fixed at zero at the same time. To gauge the dependence of both correlators on the background, similar amount of events was generated for two levels of the percentage of LCC, using 33% and 50% for Pb-system and 15% and 30% for Xe-system, but fixing n_5/s at zero this time.

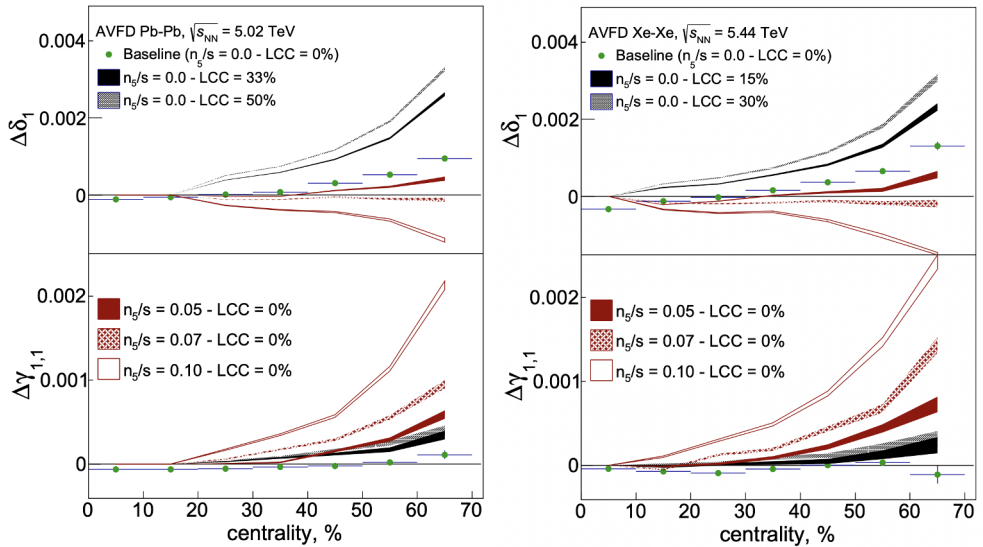


Figure 1: The centrality dependence of $\Delta\delta_1$ (upper panel) and $\Delta\gamma_{1,1}$ (lower panel) in Pb-Pb collisions at $\sqrt{s_{NN}} = 5.02$ TeV (left) and in Xe-Xe collisions at $\sqrt{s_{NN}} = 5.44$ TeV collisions (right). The results from the analysis of the baseline sample are represented by the green markers. The various bands show the AVFD expectations for $\Delta\delta_1$ and $\Delta\gamma_{1,1}$ for various values of n_5/s (red bands) and percentage of LCC (blue bands).

Figure 1 shows the centrality dependence of $\Delta\delta_1$ (upper panel) and $\Delta\gamma_{1,1}$ (lower panel) in Pb-Pb collisions at $\sqrt{s_{NN}} = 5.02$ TeV (left) and in Xe-Xe collisions at $\sqrt{s_{NN}} = 5.44$ TeV collisions (right), respectively. The baseline curves of two correlators, $\Delta\delta_1$ and $\Delta\gamma_{1,1}$, represented by green markers, exhibit non-zero values for the majority of the centrality intervals in both collision systems. These non-zero values are due to the existence of hadronic resonances in the model, whose decay products are affected by both radial and elliptic flows. Moreover, the dependence of these two correlators on various choices of the axial current density n_5/s for two collision systems is represented by the red bands. It is conspicuous that in both Pb-Pb and Xe-Xe collisions, the increase of n_5/s leads to opposite trends in the two correlators : decrease in the values of $\Delta\delta_1$ and rise in the values of $\Delta\gamma_{1,1}$. This is an expected behaviour as a consequence of the different sign in front of the CME induced contribution, $\langle a_{1,\alpha} a_{1,\beta} \rangle$, in Eqs. (1) and (2), respectively. Finally, the blue bands show the dependence of two correlators on the percentage of LCC in two collision systems when n_5/s is fixed to zero. With the increase in the percentage of LCC, both $\Delta\delta_1$ and $\Delta\gamma_{1,1}$ increase in both collision systems.

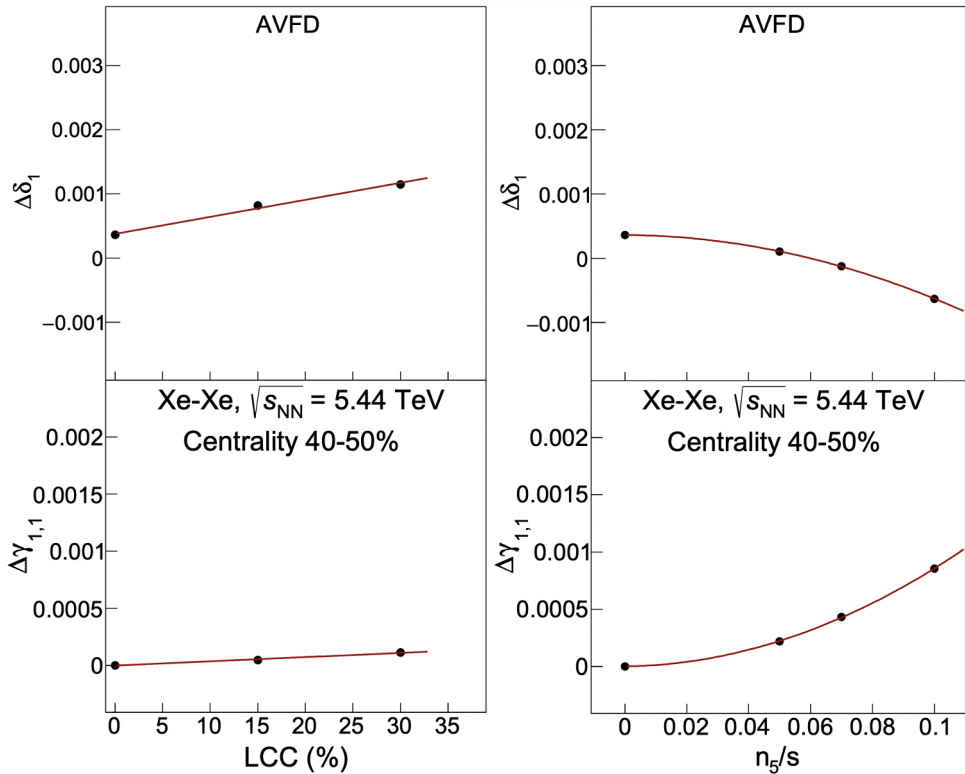


Figure 2: The dependence of $\Delta\delta_1$ and $\Delta\gamma_{1,1}$ in the upper and lower panels, respectively, on the percentage of LCC (left) and the axial current density n_5/s (right) in the analysed samples of Xe-Xe collisions at $\sqrt{s_{NN}} = 5.44$ TeV for the 40%-50% centrality interval. The black curves are the lines of parametrisation.

For each centrality interval of both collision systems, we can parametrise the dependence of each of the correlators with respect to n_5/s and the percentage of LCC. As LCC and the generation of axial current density are two independent processes happening at different

stages of heavy-ion collisions, these two effects can be parametrised individually but their combined effect should quantitatively reproduce experimentally measured $\Delta\delta_1$ and $\Delta\gamma_{1,1}$. Following this procedure, one is able to parametrise the dependence of $\Delta\delta_1$ and $\Delta\gamma_{1,1}$ according to

$$\begin{aligned}\Delta\delta_1 &= c_2 \cdot (n_5/s)^2 + c_1 \cdot (n_5/s) + b_1 \cdot (LCC) + b_0, \\ \Delta\gamma_{1,1} &= e_2 \cdot (n_5/s)^2 + e_1 \cdot (n_5/s) + d_1 \cdot (LCC) + d_0,\end{aligned}\quad (3)$$

where $e_2, e_1, d_1, d_0, c_2, c_1, b_1$ and b_0 are real numbers constrained by the simultaneous fit of the corresponding dependencies of $\Delta\delta_1$ and $\Delta\gamma_{1,1}$ for each centrality interval of every collision system and energy. In Fig. 3, the results for the 40–50% centrality interval of Xe-Xe collisions at $\sqrt{s_{NN}} = 5.44$ TeV are indicatively chosen to demonstrate the procedure. As one can see, the increase in the percentage of LCC scales with the values of $\Delta\delta_1$ and $\Delta\gamma_{1,1}$ linearly, while the dependence of $\Delta\delta_1$ and $\Delta\gamma_{1,1}$ on n_5/s is quadratic with opposite trend. The quadratic dependence and the opposite trend originate from the CME signal terms $\langle a_{1,\alpha} a_{1,\beta} \rangle$ and $-\langle a_{1,\alpha} a_{1,\beta} \rangle$ in the decomposed form of δ_1 and $\gamma_{1,1}$, as shown in Eqs. (1) and (2). The coefficient a_1 is demonstrated to be proportional to n_5/s in [17, 18].

4 Results

The parametrisation described by Eqs. (1) and (2) provides the necessary relationship to unambiguously deduce the optimum model based values of n_5/s and the percentage of LCC for each centrality, colliding system and energy, to quantitatively reproduce the centrality dependence of $\Delta\delta_1$ and $\Delta\gamma_{1,1}$ measured by the ALICE collaboration.

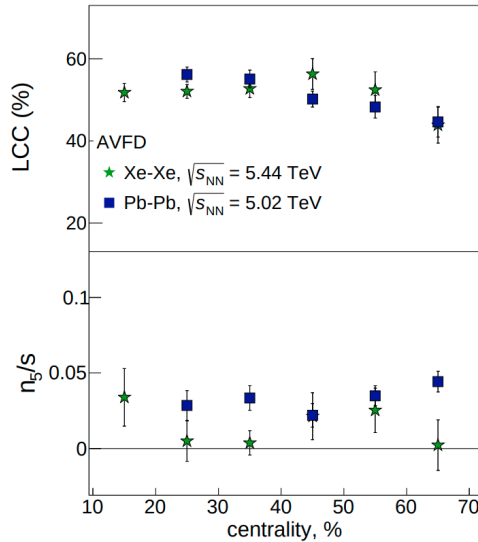


Figure 3: The centrality dependence of the LCC percentage (upper panel) and the axial current density n_5/s that allow one to describe simultaneously the experimentally measured dependencies of $\Delta\delta_1$ and $\Delta\gamma_{1,1}$ on n_5/s [10–12] in all collision systems and at all energies studied in this article.

Fig. 3 presents the final best fit values of the percentage of LCC (upper panel) and n_5/s (lower panel) at each centrality interval that are needed as input parameters for AVFD so as to

describe experimental results ($\Delta\delta_1$ and $\Delta\gamma_{1,1}$). From the upper panel, it is apparent that both collision systems can be described by large values of LCC that range from 40% for peripheral up to around 60% for more central Pb–Pb collisions. No significant difference between Pb–Pb and Xe–Xe was observed in the values of LCC percentage across all centrality intervals. The lower panel of Fig. 3 shows that n_5/s depends weakly on centrality while a dependence on colliding systems is observed. For Xe–Xe collisions, the experimental results lead to values of n_5/s compatible with zero within the uncertainties for all centrality intervals. Fitting the n_5/s values with a constant function yields 0.011 ± 0.005 as its best fit value. On the other hand, the experimentally measured correlators in Pb–Pb collisions require a non-zero input values of axial current densities in AVFD model for all centrality regions studied. The same fit with a constant function leads to a value of 0.034 ± 0.003 , which is significantly above the background-only scenario.

5 Conclusion

We utilised the Anomalous-Viscous Fluid Dynamics framework to perform a systematic study of charge-dependent azimuthal correlations measured by the ALICE collaboration for Pb–Pb and Xe–Xe collisions at $\sqrt{s_{NN}} = 5.02$ TeV and $\sqrt{s_{NN}} = 5.44$ TeV, respectively. The amount of axial current density (imbalanced quark chirality), related to the strength of the CME, is extracted through parametrisation of $\Delta\delta_1$ and $\Delta\gamma_{1,1}$ from the percentage of LCC (background effect) and n_5/s (yielding the amplitude of the CME signal) for both collision systems at each centrality interval studied. The results indicate that Xe–Xe collisions are consistent with a background-only scenario and a small but significant non-zero value of axial current density is required to match the measurements in Pb–Pb collisions.

References

- [1] D.E. Kharzeev, L.D. McLerran, H.J. Warringa, Nucl. Phys. A **803**, 227 (2008), 0711.0950
- [2] D. Kharzeev, R.D. Pisarski, M.H.G. Tytgat, Phys. Rev. Lett. **81**, 512 (1998), hep-ph/9804221
- [3] K. Fukushima, D.E. Kharzeev, H.J. Warringa, Phys. Rev. D **78**, 074033 (2008), 0808.3382
- [4] D.E. Kharzeev, Annals Phys. **325**, 205 (2010), 0911.3715
- [5] V. Skokov, A.Y. Illarionov, V. Toneev, Int. J. Mod. Phys. A **24**, 5925 (2009), 0907.1396
- [6] Y. Zhong, C.B. Yang, X. Cai, S.Q. Feng, Adv. High Energy Phys. **2014**, 193039 (2014), 1408.5694
- [7] G. Inghirami, M. Mace, Y. Hirono, L. Del Zanna, D.E. Kharzeev, M. Bleicher, Eur. Phys. J. C **80**, 293 (2020), 1908.07605
- [8] S.A. Voloshin, Phys. Rev. C **70**, 057901 (2004), hep-ph/0406311
- [9] K. Aamodt et al. (ALICE), Phys. Rev. Lett. **106**, 032301 (2011), 1012.1657
- [10] S. Acharya et al. (ALICE), JHEP **09**, 160 (2020), 2005.14640
- [11] S. Aziz (ALICE), Nucl. Phys. A **1005**, 121817 (2021), 2005.06177
- [12] (2022), 2210.15383
- [13] B.I. Abelev et al. (STAR), Phys. Rev. Lett. **103**, 251601 (2009), 0909.1739
- [14] B.I. Abelev et al. (STAR), Phys. Rev. C **81**, 054908 (2010), 0909.1717
- [15] S. Schlichting, S. Pratt, Phys. Rev. C **83**, 014913 (2011), 1009.4283
- [16] S. Pratt, S. Schlichting, S. Gavin, Phys. Rev. C **84**, 024909 (2011), 1011.6053

- [17] S. Shi, Y. Jiang, E. Lilleskov, J. Liao, *Annals Phys.* **394**, 50 (2018), 1711.02496
- [18] S. Shi, Y. Jiang, E. Lilleskov, Y. Yin, J. Liao, *Nucl. Phys. A* **967**, 748 (2017), 1704.05531
- [19] S. Shi, H. Zhang, D. Hou, J. Liao, *Phys. Rev. Lett.* **125**, 242301 (2020), 1910.14010
- [20] P. Christakoglou, S. Qiu, J. Staa, *Eur. Phys. J. C* **81**, 717 (2021), 2106.03537